


 Cite this: *Chem. Commun.*, 2023, 59, 5387

 Received 28th February 2023,  
 Accepted 11th April 2023

DOI: 10.1039/d3cc01007d

rsc.li/chemcomm

# Combining ligand-enhanced backdonation and steric shielding to stabilize a mono-substituted Au(I) carbene<sup>†</sup>

 David Vesseur,<sup>a</sup> Karinne Miqueu <sup>b</sup> and Didier Bourissou <sup>\*a</sup>

A mono-substituted Au(I) carbene was prepared by reacting HC(N<sub>2</sub>)(Dmp) (Dmp = 2,6-dimesitylphenyl) with an (*o*-carboranyl)-diphosphine AuNTf<sub>2</sub> complex. It is stable up to −10 °C and was characterized by NMR spectroscopy. According to DFT calculations, the chelating P^P ligand enhances Au → C<sub>carb</sub> backdonation, while the Dmp substituent provides kinetic stabilization but does not bias the electronic structure of the carbene complex.

Many catalytic transformations involve gold(I) carbene complexes as key intermediates and these species attract considerable attention.<sup>1</sup> Important synthetic efforts have been devoted to the preparation and characterization of [L<sub>n</sub>Au=C<]<sup>+</sup> complexes<sup>2</sup> with various substitution patterns at the carbenic center (with and without heteroelements) and various ancillary ligands at gold (from phosphines, *N*-heterocyclic carbenes to diphosphines). See Chart 1 for representative examples of recently isolated and/or spectroscopically characterized compounds. The nature of the AuC<sub>carb</sub> bonds also raises fundamental questions, with the cationic gold carbene Au<sup>+</sup>=C< and metala-carbocationic (carbenoid) Au–C<<sup>+</sup> structures as limit canonical forms.<sup>3</sup> Most of the gold(I) carbene complexes reported so far are disubstituted, but in 2019, Echavarren *et al.* were able to observe monosubstituted gold(I) carbenes by NMR at −90 °C.<sup>4</sup> Here, gold bears JohnPhos-type ligands and the carbene center is substituted by a mesityl (Mes) group. These species are stable only until −70 °C, but display rich reactivity.<sup>5</sup>

Over the past few years, our group has demonstrated that (*o*-carboranyl)-diphosphines are very efficient in enhancing backdonation from gold (thanks to P^P chelation) and stabilizing disubstituted gold(I) carbenes.<sup>2c,6</sup> In this work, we envisioned to combine this approach with kinetic stabilization by a sterically demanding substituent. Hereafter, we report our first results along this line. A monosubstituted gold(I) carbene stable up to −10 °C has been prepared and characterized by multi-nuclear NMR spectroscopy. Its bonding situation was analysed computationally.

As sterically demanding aryl substituent, we choose the 2,6-dimesitylphenyl (Dmp) moiety which has been successfully employed by Hillhouse *et al.* to prepare low coordinate Ni complexes, (NHC)Ni(Dmp) and (P^P)Ni = CH(Dmp) species in particular.<sup>7,8</sup> The 2,6-dimesitylphenyl diazomethane HC(N<sub>2</sub>)Dmp was prepared in 4 steps from mesityl bromide and 1,3-dichlorobenzene in an overall yield of 32%.<sup>9</sup> The reported synthesis<sup>8a</sup> was modified and improved by replacing the highly toxic hydrazine and mercuric oxide for tosylhydrazine and sodium hydride.

Adding the pseudo-cationic (P^P)AuNTf<sub>2</sub> complex<sup>10</sup> to HC(N<sub>2</sub>)Dmp at −50 °C in dichloromethane resulted in a quick

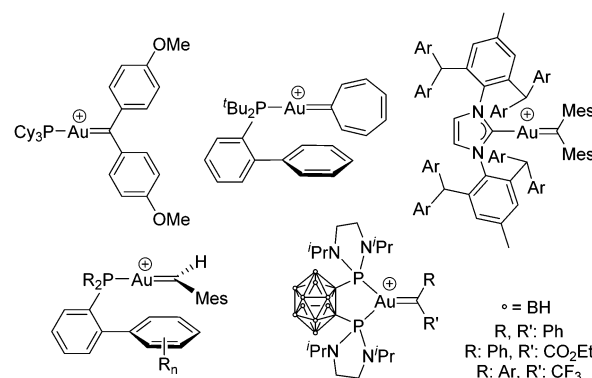


Chart 1 Representative examples of recently isolated and/or spectroscopically characterized [L<sub>n</sub>Au=C<]<sup>+</sup> complexes.

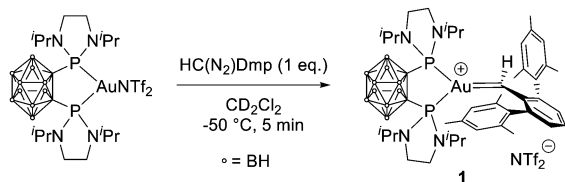
<sup>a</sup> Laboratoire Hétérochimie Fondamentale et Appliquée, Université Paul Sabatier/ CNRS UMR 5069, 118 Route de Narbonne, Toulouse Cedex 09 31062, France.

E-mail: didier.bourissou@univ-tlse3.fr

<sup>b</sup> CNRS/Université de Pau et des Pays de l'Adour, E2S UPPA, Institut des Sciences Analytiques et de Physico-Chimie pour l'Environnement et les Matériaux (IPREM, UMR 5254), Hélioparc, 2 Avenue du Président Angot, Pau Cedex 09 64053, France

<sup>†</sup> Electronic supplementary information (ESI) available: Experimental procedures, characterization of complex 1, computational data (PDF). See DOI: <https://doi.org/10.1039/d3cc01007d>





**Scheme 1** Reaction of  $(P^P)AuNTf_2$  with  $HC(N_2)Dmp$  resulting in the monosubstituted carbene **1**.

colour change from pale yellow-orange to deep purple (Scheme 1).

The monosubstituted carbene **1** was characterized by low-temperature multi-nuclear NMR spectroscopy (at  $-80\text{ }^\circ\text{C}$ ).<sup>9</sup> A single peak at  $\delta$  141.3 ppm was observed in the  $^{31}\text{P}$  NMR spectrum, indicating a clean and quantitative reaction. The  $^1\text{H}$  NMR spectrum shows a triplet at  $\delta$  13.36 ppm ( $J_{\text{HP}} = 16.6\text{ Hz}$ ) for the  $AuCH(Dmp)$  moiety (Fig. 1). This is approximately 1 ppm downfield shifted compared to the corresponding signal reported previously for the  $(\text{JohnPhos})AuCH(\text{Mes})^+$  complexes ( $\delta$  11.74–12.67 ppm).<sup>4</sup> The  $^{13}\text{C}$  NMR resonance at  $\delta$  295.6 ppm (triplet,  $J_{\text{CP}} = 85.6\text{ Hz}$ ) is also very diagnostic for the carbene complex **1**. It matches well with those found for the monosubstituted carbenes ( $\delta$  284.6–290.0 ppm).<sup>4</sup> The correlation observed between the carbenic carbon and proton signals upon  $^1\text{H}$ – $^{13}\text{C}$  HSQC analysis further confirms the assignment. The  $^1\text{H}$  and  $^{13}\text{C}$  resonances associated with the Dmp moiety were assigned thanks to HSQC and HMBC experiments. The two mesityl groups were found to be inequivalent (two sets of signals were observed), indicating hindered rotation around the  $Au=C(H)(Dmp)$  bond.

The thermal stability of **1** was then investigated. No colour change was observed when the  $(P^P)AuNTf_2$  complex was added to  $HC(N_2)Dmp$  at  $-80\text{ }^\circ\text{C}$ . When the solution was warmed, the characteristic purple colour appeared at *ca.*  $-60\text{ }^\circ\text{C}$  and then disappeared at *ca.*  $-10\text{ }^\circ\text{C}$ . A variable temperature NMR monitoring was then carried out. A freshly prepared sample of **1** was analysed from  $-80\text{ }^\circ\text{C}$  to room temperature by intervals of  $10\text{ }^\circ\text{C}$ .<sup>9</sup> Accordingly, carbene **1** was found to survive up to  $-10\text{ }^\circ\text{C}$  and to degrade completely within 5 minutes at  $0\text{ }^\circ\text{C}$ . The thermal stability of complex **1** substantiates the combined effect of  $Au \rightarrow C_{\text{carb}}$  backdonation (enhanced by the  $P^P$  ligand) and steric shielding (imparted by the Dmp substituent). The  $(\text{JohnPhos})AuCH(\text{Mes})^+$  complexes could be spectroscopically characterized at low temperature, but they were shown to decompose at temperatures between  $-90$  and  $-70\text{ }^\circ\text{C}$ .<sup>4</sup>

Despite our efforts, attempts to grow crystals suitable for XRD remained unsuccessful. To gain more insight into the structure and bonding situation of the  $(P^P)Au=CH(Dmp)^+$  complex, Density Functional Theory (DFT) calculations were carried out. The actual compound was considered, without simplification of the substituents, but the counter-anion was omitted. It is referred hereafter as **A-Dmp**. The B3PW91/SDD+f(Au), 6-31G\*\* (other atoms) level of theory was used to enable comparison with related complexes. The optimized structure (Fig. 2, left) shows a tricoordinate gold complex (the two P atoms chelate the metal with a bite angle close to  $90^\circ$ ). The carbene center sits in a planar environment which substantially deviates from trigonal due to the dissymmetric substitution pattern. The  $AuC_{\text{carb}}H$  bond angle is contracted while the  $AuC_{\text{carb}}C_{\text{ipso}}$  bond angle is widened at *ca.*  $108$  and  $144^\circ$ ,

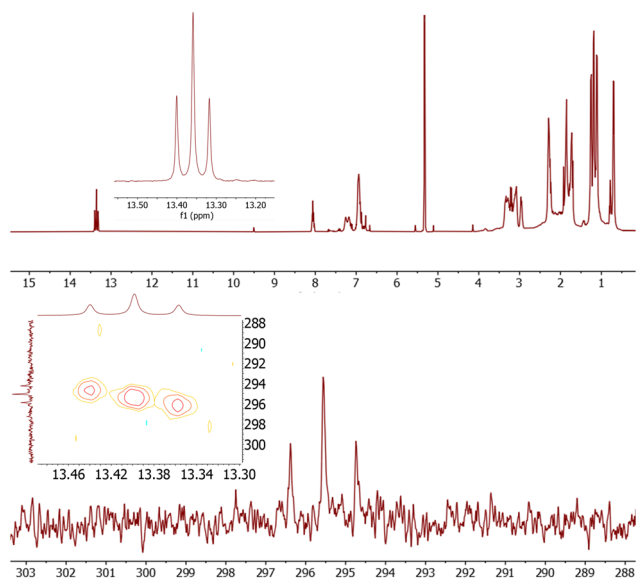


**Fig. 1** Top:  $^1\text{H}$  NMR (400.13 MHz) spectrum of **1** with the  $Au=CH$  signal as inset. Bottom:  $^{13}\text{C}$  NMR (100.63 MHz) carbenic signal of **1** with the corresponding  $^1\text{H}$ – $^{13}\text{C}$  HSQC correlation as inset. Spectra recorded in  $CD_2Cl_2$  at  $-80\text{ }^\circ\text{C}$ .

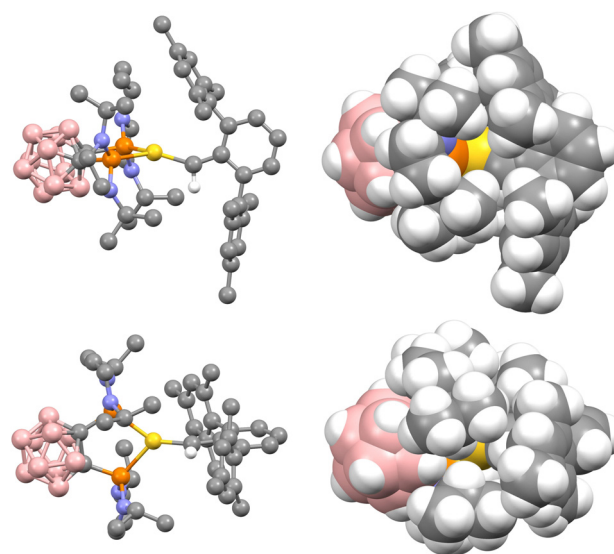
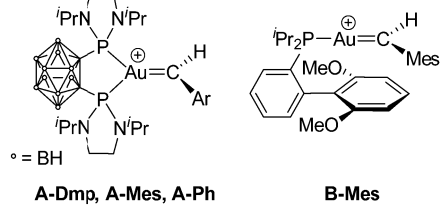


**Fig. 2** Optimized geometry (left) and space filling model (right) for the  $(P^P)Au=CH(Dmp)^+$  complex **A-Dmp** at the B3PW91/SDD+f(Au), 6-31G\*\* (other atoms) level of theory. Front (top) and side (bottom) views. Boron in pink, Phosphorus in orange, Nitrogen in blue, Gold in yellow, Carbon in grey, Hydrogen in white. For clarity, the hydrogen atoms are omitted in the optimized structures, except the one at the carbene center.



**Table 1** Key geometric features (bond distances in Å, bond angles in °) and bonding data computed for the (P<sup>^</sup>P)AuCH(Ar)<sup>+</sup> complexes (Ar = Dmp, Mes, Ph) **A-Dmp**, **A-Mes**, **A-Ph**, as well as the reference (Johnphos)Au=CH(Mes)<sup>+</sup> complex **B-Mes**



	A-Dmp	A-Mes	A-Ph	B-Mes
<b>Optimized structures</b>				
Au=C <sub>carb</sub>	1.975	1.979	1.959	2.007
PAu	2.458	2.429	2.422	2.378
	2.456	2.441	2.427	
C <sub>carb</sub> -C <sub>ipso</sub>	1.428	1.417	1.429	1.400
PAuP	88.94	89.44	89.14	—
AuCH	107.95	110.30	115.37	110.32
AuCC <sub>ipso</sub>	143.76	138.55	133.04	138.51
AuCC <sub>ipso</sub> C <sub>ortho</sub>	1.0	-5.0	1.2	-5.4
<b>NBO analyses</b>				
WBI(AuC <sub>carb</sub> )	0.754	0.727	0.768	0.681
WBI(C <sub>ipso</sub> C <sub>ortho</sub> )	1.294	1.344	1.128	1.438
CT	-0.03	-0.02	-0.09	0.27
<b>CDA analyses</b>				
C <sub>carb</sub> → Au donation	0.482	0.447	0.365	0.391
Au → C <sub>carb</sub> backdonation	0.231	0.215	0.219	0.119
d/b ratio	2.09	2.08	1.67	3.29

respectively (Table 1). The carbene plane is about perpendicular to the Au coordination plane, to minimize steric repulsions and maximize Au → C<sub>carb</sub> backdonation. Conversely, the phenyl ring of the Dmp moiety is coplanar with the carbene to accommodate the *o,o'*-Mes groups and enable π-donation to the vacant 2p<sup>π</sup>(C<sub>carb</sub>) orbital. The Au=C<sub>carb</sub> bond length (1.975 Å) is comparable to those found in disubstituted (P<sup>^</sup>P)Au=C(R)(R')<sup>+</sup> complexes.<sup>6</sup> The C<sub>carb</sub>-C<sub>ipso</sub> bond length (1.428 Å) is similar to those found in (P<sup>^</sup>P)AuC(CF<sub>3</sub>)(Ar)<sup>+</sup> complexes, suggesting some π-stabilization of the carbene center.<sup>6c</sup> The P<sup>^</sup>P ligand at gold and the Dmp substituent provide huge steric shielding. The central Au=CH moiety is protected by the P substituents on one side and the flanking Mes groups of the Dmp substituent on the other side, as apparent from the space filling model (Fig. 2, right).

Inspection of the frontier orbitals shows some Au=C<sub>carb</sub> π-bonding as the result of Au → C<sub>carb</sub> backdonation (Fig. 3). The HOMO/LUMO correspond mainly to bonding/anti-bonding combinations between an in-plane d(Au) orbital and the vacant 2p<sup>π</sup>(carbene) orbital. The HOMO/LUMO energy gap (2.64 eV) is comparable to those found in disubstituted (P<sup>^</sup>P)Au=C(R)(R')<sup>+</sup> carbenes (2.34–2.58 eV).<sup>6</sup> In addition, a Natural Localized Molecular Orbital (NLMO) associated to the Au → C<sub>carb</sub> backdonation evidences non-negligible mixing of the 2p<sup>π</sup>(C<sub>carb</sub>) orbital with the d(Au)-centered orbital (9.1% C<sub>carb</sub>), in line with some Au=C<sub>carb</sub> π-bonding.<sup>9</sup>

To further gauge the AuC<sub>carb</sub> bonding, Natural Bond Orbital (NBO) analyses, Energy and Charge Decomposition Analyses (EDA and CDA) were performed (Table 1 and Table S4, ESI<sup>†</sup>).<sup>9</sup> Accordingly, the interaction between (P<sup>^</sup>P)Au<sup>+</sup> and CH(Dmp)

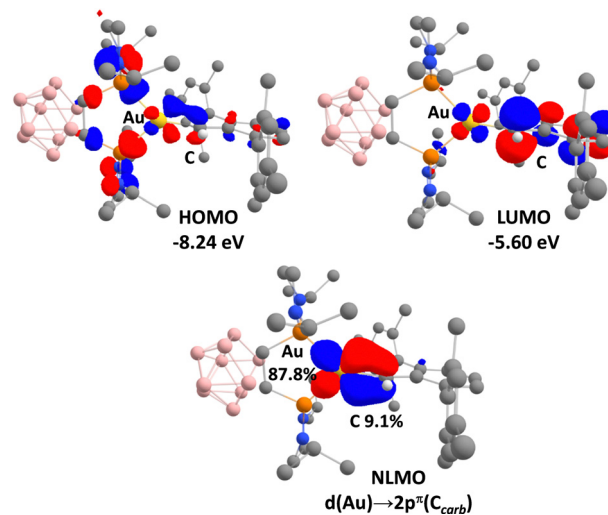


**Fig. 3** Frontier orbitals (cutoff: 0.05) computed for the (P<sup>^</sup>P)Au=CH(Dmp)<sup>+</sup> complex **A-Dmp** at the B3PW91/SDD+f(Au), 6-31G\*\* (other atoms) level of theory. NLMO (cutoff: 0.04) associated to the Au → C<sub>carb</sub> backdonation with contribution in % of Au and C<sub>carb</sub> atoms.

(both in the singlet state) turned to be the best fragmentation to describe **A-Dmp**. The charge transfer (CT) from the carbene center to the metal fragment was found close to zero (-0.03 e), while the donation/backdonation ratio (2.09) indicates the predominance of C<sub>carb</sub> → Au donation, with significant Au → C<sub>carb</sub> backdonation however.

We then questioned whether the steric shielding of the Dmp substituent influences the bonding situation or not. We tried to prepare the related (P<sup>^</sup>P)Au=CH(Mes)<sup>+</sup> complex by the same route, *i.e.* reacting (P<sup>^</sup>P)Au(NTf<sub>2</sub>) with HC(N<sub>2</sub>)Mes. In this case, only diazo decomposition was observed and no gold carbene could be characterized. The carbenoid route employed by Echavarren *et al.*<sup>4</sup> to access the (JohnPhos)AuCH(Ar)<sup>+</sup> complexes was also tested but we could not find suitable conditions for the formal insertion of the carbene into the Au-Cl bond of the (P<sup>^</sup>P)AuCl complex. Mixing (P<sup>^</sup>P)AuCl with HC(N<sub>2</sub>)Mes only led to decomposition of the gold complex.<sup>11</sup>

We thus resorted to DFT and performed calculations on the (P<sup>^</sup>P)Au=CH(Mes)<sup>+</sup> and (P<sup>^</sup>P)Au=CH(Ph)<sup>+</sup> complexes, **A-Mes** and **A-Ph**, respectively (Table 1). No significant difference was noticed between the optimized geometries of **A-Dmp**, **A-Mes** and **A-Ph**. The MO, NBO and CDA analyses also reveal very similar bonding situations. Thus, the huge steric hindrance of the Dmp substituent provides kinetic stabilization but does not bias the electronic structure of the carbene complex. Comparison with the complex **B-Mes** bearing a JohnPhos-type ligand is also insightful. The key geometric features do not differ much, but it is worth noting that the Au=C<sub>carb</sub> bond is longer (2.007 Å) while the C<sub>carb</sub>-C<sub>ipso</sub> bond length is slightly shorter (1.400 Å). This suggests weaker Au → C<sub>carb</sub> backdonation and stronger Ar → C<sub>carb</sub> π-donation in **B-Mes** than in **A-Dmp**, as further supported by the respective Wiberg Bond Indexes (WBI). The CT value (0.27 e) and d/b ratio (3.29) found for **B-Mes** by NBO and CDA confirm this view and highlight the Au → C<sub>carb</sub> backdonation enhancement induced by the chelating P<sup>^</sup>P ligand.



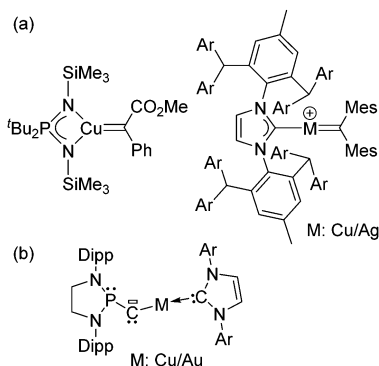


Chart 2 Representative examples of (a) copper/silver carbene complexes and (b) metalla carbene/carbyne complex recently authenticated.

In conclusion, a monosubstituted gold(I) carbene stable up to  $-10\text{ }^{\circ}\text{C}$  has been prepared thanks to the combined use of a chelating (*o*-carboranyl)-diphosphine ligand, to enhance  $\text{Au} \rightarrow \text{C}_{\text{carb}}$  backdonation, and the sterically demanding Dmp substituent, to provide kinetic stabilization.

Future work will aim to extend this approach to other fleeting carbene complexes. Besides gold, it may be applicable to copper and silver, for which only few carbene complexes have been authenticated so far (Chart 2a).<sup>12</sup> Other exciting targets are the low valent complexes  $L_n\text{MCR}$  for which representatives of both the metalla carbene form and the carbyne complex have been recently reported (Chart 2b).<sup>13</sup>

Financial support from the Centre National de la Recherche Scientifique and the Université de Toulouse is gratefully acknowledged. The NMR service of ICT (Pierre Lavedan) is acknowledged for assistance with the variable-temperature NMR experiments. The “Direction du Numérique” of the Université de Pau et des Pays de l’Adour and Mésocentre de Calcul Intensif Aquitain (MCIA) are acknowledged for the support of computational facilities. This work was also granted access to the HPC resources of IDRIS under the allocation 2022-[AD010800045R1] made by GENCI. Laura Estévez is thanked for preliminary DFT calculations.

## Conflicts of interest

There are no conflicts to declare.

## Notes and references

- (a) D. Qian and J. Zhang, *Chem. Soc. Rev.*, 2015, **44**, 677–698; (b) L.-W. Ye, X.-Q. Zhu, R. L. Sahani, Y. Xu, P.-C. Qian and R.-S. Liu, *Chem. Rev.*, 2021, **121**, 9039–9112; (c) T. Wang and A. S. K. Hashmi, *Chem. Rev.*, 2021, **121**, 8948–8978.
- (a) R. J. Harris and R. A. Widenhoefer, *Chem. Soc. Rev.*, 2016, **45**, 4533–4551; (b) R. Peloso and E. Carmona, *Coord. Chem. Rev.*, 2018, **355**, 116–132; (c) M. Navarro and D. Bourissou, *Adv. Organomet. Chem.*, 2021, **76**, 101–144.
- (a) D. Benitez, N. D. Shapiro, E. Tkatchouk, Y. Wang, W. A. Goddard III and F. D. Toste, *Nat. Chem.*, 2009, **1**, 482–486; (b) Y. Wang, M. E. Muratore and A. M. Echavarren, *Chem. – Eur. J.*, 2015, **21**, 7332–7339; (c) L. Nunes dos Santos Comprido, J. E. M. N. Klein, G. Knizia, J. Kästner and A. S. K. Hashmi, *Angew. Chem., Int. Ed.*, 2015, **54**, 10336–10340; (d) R. P. Herrera and M. C. Gimeno, *Chem. Rev.*, 2021, **121**, 8311–8363.
- C. García-Morales, X.-L. Pei, J. M. Sarria Toro and A. M. Echavarren, *Angew. Chem., Int. Ed.*, 2019, **58**, 3957–3961.
- Gold(I) sulfonium benzyliide complexes  $[(\text{JohnPhos})\text{AuCH}(\text{SR}^1\text{R}^2)\text{Ph}]^+$  have also been reported and shown to undergo carbene transfer reactions: (a) R. G. Carden and R. A. Widenhoefer, *Chem. – Eur. J.*, 2019, **47**, 11026–11030; (b) M. Rivers, R. G. Carden and R. A. Widenhoefer, *Organometallics*, 2022, **41**, 1106–1114.
- (a) M. Joost, L. Estévez, S. Mallet-Ladeira, K. Miqueu, A. Amgoune and D. Bourissou, *Angew. Chem., Int. Ed.*, 2014, **53**, 14512–14516; (b) A. Zeineddine, F. Rekhroukh, E. D. Sosa Carrizo, S. Mallet-Ladeira, K. Miqueu, A. Amgoune and D. Bourissou, *Angew. Chem., Int. Ed.*, 2018, **57**, 1306–1310; (c) M. Rigoulet, D. Vasseur, K. Miqueu and D. Bourissou, *Angew. Chem., Int. Ed.*, 2022, **61**, e202204781.
- (a) C. A. Laskowski, D. J. Bungum, S. M. Baldwin, S. A. Del Ciello, V. M. Iluc and G. L. Hillhouse, *J. Am. Chem. Soc.*, 2013, **135**, 18272–18275; (b) V. M. Iluc and G. L. Hillhouse, *J. Am. Chem. Soc.*, 2014, **136**, 6479–6488.
- Other examples using the bulky Dmp moiety for stabilization include  $\alpha$ -diazoalkyl Cu(I) complexes and a terminally nitrogen coordinated Co(0) diazo complex: (a) V. M. Iluc, C. A. Laskowski and G. L. Hillhouse, *Organometallics*, 2009, **28**, 6135–6138; (b) J. Du, W. Chen, Q. Chen, X. Leng, Y.-S. Meng, S. Gao and L. Deng, *Organometallics*, 2020, **39**, 729–739.
- See ESI† for details.
- M. Joost, A. Zeineddine, L. Estévez, S. Mallet-Ladeira, K. Miqueu, A. Amgoune and D. Bourissou, *J. Am. Chem. Soc.*, 2014, **136**, 14654–14657.
- The reaction was tried in toluene and dichloromethane at room temperature and  $40\text{ }^{\circ}\text{C}$ .
- (a) B. F. Straub and P. Hofmann, *Angew. Chem., Int. Ed.*, 2001, **40**, 1288–1290; (b) M. W. Hussong, W. T. Hoffmeister, F. Rominger and B. F. Straub, *Angew. Chem., Int. Ed.*, 2015, **54**, 10331–10335; (c) M. Álvarez, M. Besora, F. Molina, F. Maseras, T. R. Belderrain and P. J. Pérez, *J. Am. Chem. Soc.*, 2021, **143**, 4837–4843.
- (a) C. Hu, X.-F. Wang, R. Wei, C. Hu, D. A. Ruiz, Y.-Y. Chang and L. L. Liu, *Chemistry*, 2022, **8**, 2278–2289; (b) R. Wei, X.-F. Wang, C. Hu and L. L. Liu, *Nat. Synth.*, 2023, **2**, 357–363.

